Solar-blind $Al_xGa_{1-x}N$-based avalanche photodiodes

Turgut Tut, Serkan Butun, Bayram Butun, Mutlu Gokkavas, HongBo Yu, and Ekmel Ozbay
Nanotechnology Research Center, Bilkent University, Bilkent, 06800 Ankara, Turkey

(Received 11 October 2005; accepted 18 October 2005; published online 21 November 2005)

We report the Metalorganic Chemical Vapor Deposition (MOCVD) growth, fabrication, and characterization of solar blind $Al_xGa_{1-x}N$/GaN-based avalanche photodiodes. The photocurrent voltage characteristics indicate a reproducible avalanche gain higher than 25 at a 72 V applied reverse bias. Under a 25 V reverse bias voltage, the 100 μm diameter devices had a maximum quantum efficiency of 55% and a peak responsivity of 0.11 A/W at 254 nm, and a NEP of $1.89\text{x}10^{-16}$ W/Hz$^{1/2}$. © *2005 American Institute of Physics*. [DOI: 10.1063/1.2135952]

The recent developments in GaN/AlGaN material growth technology have led to the fabrication of high performance photodetectors operating in the UV spectral region. AlGaN-based Schottky,[1,2] *p-i-n*[3,4] and MSM[5] photodetectors with excellent detectivity performances have been reported. However, very few GaN-based avalanche photodiodes (APDs) were reported in the literature,[6–11] and there are not any publications reporting AlGaN-based APDs. The high defect densities in the epitaxial layers grown on lattice-mismatched substrates result in a premature microplasma breakdown before the electric field can reach the bulk avalanche breakdown level, which is a major problem for the AlGaN/GaN APDs.[8,11] In this paper, we report the epitaxial growth, fabrication, and characterization of AlGaN-based APDs operating in the solar-blind spectral region.

The epitaxial structure of the front-illumination Schottky detector wafer was designed to achieve true-solar blindness, very low dark current, high solar rejection, and high breakdown. Low leakage and high breakdown are needed in order to see the avalanche effect. The $Al_{0.38}Ga_{0.62}N$ absorption layer was used to achieve $\lambda_c < 280$ nm. The $Al_xGa_{1-x}N$/GaN epitaxial layers of our heterojunction Schottky photodiode wafer were grown on a 2 in. single-side polished (0001) sapphire substrate using the Aixtron 200/4 RF-S MOCVD system located at the Bilkent University Nanotechnology Research Center. A thin AlN nucleation layer and a subsequent 0.5 μm thick unintentionally doped GaN mesa isolation layer was first grown. This was followed by the growth of a highly doped ($n^+ = 2\times10^{18}$ cm^{-3})0.6 μm thick GaN Ohmic contact layer and a 0.2 μm thick $Al_{0.38}Ga_{0.62}N$ layer at the same doping level. The epitaxial growth of the wafer was completed with the deposition of a 0.8 μm thick undoped $Al_{0.38}Ga_{0.62}N$ active layer. The highly doped GaN layer was used for the Ohmic contact region due to the difficulty of obtaining high-quality Ohmic contacts with $Al_xGa_{1-x}N$ layers. The *n*-type doped 0.2 μm thick $Al_{0.38}Ga_{0.62}N$ layer was used as a diffusion barrier for the photocarriers generated in the GaN Ohmic contact layer. Such a diffusion barrier is expected to increase the solar-blind/near-UV rejection ratio of the detector.

The samples were fabricated by using a five-step microwave-compatible fabrication process in a class-100 clean room environment. First, the Ohmic contact regions were defined via reactive ion etching (RIE) under CCl_2F_2 plasma, a 20 sccm gas flow rate, and 100W rf power. The etch rates for the GaN and $Al_{0.38}Ga_{0.62}N$ layers were 326 and 178 Å/min., respectively. After an Ohmic etch of $\sim$1.2 μm, Ti/Al(100 Å/1000 Å) contacts were deposited via thermal evaporation and left in an acetone solution for the lift-off process. The contacts were annealed at 650 °C for 60 s in a rapid thermal annealing system. A $\sim$100 Å thick Au film was evaporated in order to form Au/AlGaN Schottky contacts. Mesa structures of the devices were formed via the same RIE process, by etching all of the layers ($>2.1\mu$m) down to the sapphire substrate layer for better mesa isolation. Then, a 200 nm thick Si_3N_4 was deposited via plasma-enhanced chemical vapor deposition (PECVD) for passivation. Finally, a $\sim$0.6 μm thick Ti/Au interconnect metal was deposited and lifted off to connect the Schottky layers to the coplanar waveguide transmission line pads.

The resulting devices had breakdown voltages higher than 50 V. To obtain better isolation, we etched down to the sapphire substrate, which enabled us to obtain lower leakage current than previous fabrications. Figure 1 shows the dark current of a 60 μm diameter device. Dark current density at a 5 V reverse bias was 5.3×10^{-11}A/cm^2. Up to 10 V, the dark current was less than 10 fA. At 50 V bias, the device had a dark current $\sim$2 nA. The low dark current values proved the high growth quality of an AlGaN wafer with low dislocation densities. The differential resistance of our detectors at zero bias was in excess of 1.88×10^{15} Ω in the 0–20 V range.

Figure 2(a) shows the current-voltage characteristics of a device with a 100 μm diameter. The device showed almost unity-gain behavior for voltages between 10 and 50 V, and the photocurrent was approximately 10 nA. After 50 V, avalanche gain has been observed from the device. As shown in Fig. 2(b), the maximum reproducible avalanche gain was 25 at 72 V reverse bias. The onset avalanche gain field was

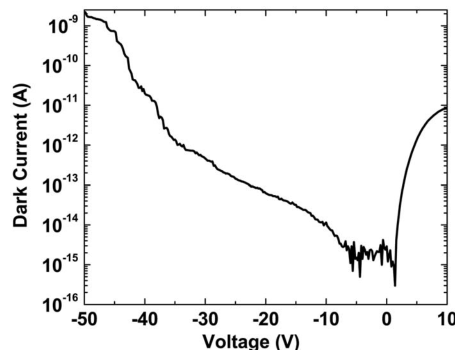

FIG. 1. Dark current of a 60 μm diameter photodetector.

0003-6951/2005/87(22)/223502/3/$22.50

© 2005 American Institute of Physics
Downloaded 23 Nov 2005 to 139.179.96.116. Redistribution subject to AIP license or copyright, see http://apl.aip.org/apl/copyright.jsp

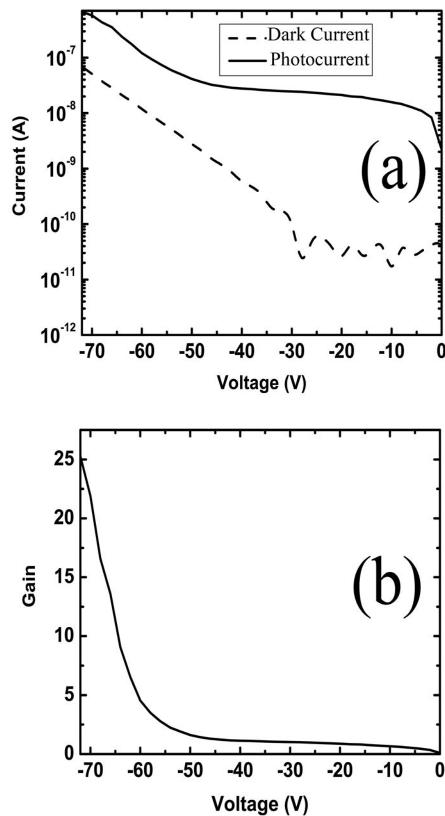

FIG. 2. (a) Dark current and photocurrent measurement of a 100 micron diameter photodetector. (b) Corresponding avalanche gain of the same device.

estimated to be approximately 1 MV/cm. Although we had observed avalanche gains as high as 200 (at ~85 V reverse bias) from some of the devices, the performance of these devices degraded rapidly after the measurements.

Figure 3(a) shows the quantum efficiency measurements of a 100 μm diameter device for different bias voltages. Under a 25 V reverse bias voltage, the device had a maximum quantum efficiency of 55% at 254 nm. The cut off wavelength was ~270 nm for all measurements. Figure 3(b) shows the responsivity measurements of the same photodetector. The peak responsivity was 0.11 A/W at a wavelength of 254 nm. The device had a rejection ratio of more than four orders of magnitude with wavelengths larger than 362 nm at a 25 V reverse bias. Using the thermal-noise-limited detectivity (D^*) formula $D^*=R_\lambda(R_0A/4kT)^{1/2}$, where R_λ is the device responsivity at zero bias, R_0 is the zero volt dark impedance, and A is the detector area, D^* is found as 4.68×10^{13} cm Hz$^{1/2}$/W, which is higher than our earlier results.[2] The corresponding noise-equivalent power (NEP) is 1.89×10^{-16} W/Hz$^{1/2}$.

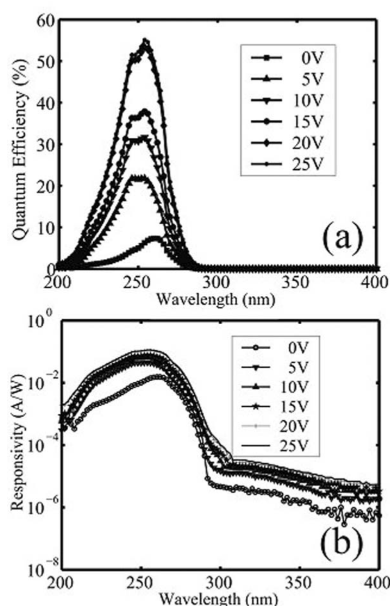

FIG. 3. (a) Quantum efficiency measurements of a 100 μm diameter photodetector. (b) Responsivity measurement of the same device in a semilog scale.

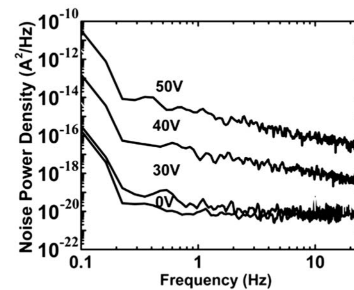

FIG. 4. Spectral noise measurement of a high-leakage 100 μm diameter photodetector with a varying applied reverse bias.

Finally, the noise characterization of the solar-blind detectors was carried out using a fast Fourier transform spectrum analyzer, current amplifier, dc voltage source, and a microwave probe station. In the 1 Hz–10 kHz range, our low-leakage, high breakdown voltage solar-blind photodetectors had noise power densities below the resolution level of the instrument. Even under 30 V, the detector noise did not exceed the measurement setup noise floor of 3×10^{-29} A^2/Hz at 10 kHz. Therefore, we measured devices with higher leakage currents in order to observe the bias dependence of the spectral noise density. We took a 100 μm diameter device that has higher dark current (5×10^{-7} A at 35 V) and a lower breakdown voltage near 50 V. As can be seen in Fig. 4, $1/f$ (flicker) noise is the dominant noise mechanism in our detectors. $1/f$ noise is known to result from contamination and crystal imperfection. Up to 30 V reverse bias voltage, the noise power density is nearly the same. At a 0 V bias voltage and 10 Hz, $S_n(f)$ is ~9.8×10^{-21} A^2/Hz, at 30 V bias it is only ~3×10^{-20} A^2/Hz, and at 50 V it is ~1.4×10^{-16} A^2/Hz. The noise curves obey the $S_n=S_0/f^b$ relation. S_0 depends on current, which is why the noise increases with an applied bias voltage in low frequencies.

In summary, we report the first solar-blind AlGaN-based avalanche photodiodes with low dark current, low noise, and high detectivity. The photocurrent-voltage characteristics indicated a reproducible gain of >25 at 72 V. The devices exhibited a maximum quantum efficiency of 55% and a peak responsivity of 0.11 A/W at a wavelength of 254 nm.

[1] A. Osinsky, S. Gangopadhyay, B. W. Lim, M. Z. Anwar, M. A. Khan, D. V. Kuksenkov, and H. Temkin, Appl. Phys. Lett. **72**, 742 (1998).
[2] T. Tut, N. Biyikli, I. Kimukin, T. Kartaloglu, O. Aytur, M. S. Unlu, and E. Ozbay, Solid-State Electron. **49**, 117 (2005).
[3] U. Chowdhury, M. M. Wong, C. J. Collins, B. Yang, J. C. Denyszyn, J. C. Campbell, and D. Dupuis, J. Cryst. Growth **248**, 552 (2003).

Downloaded 23 Nov 2005 to 139.179.96.116. Redistribution subject to AIP license or copyright, see http://apl.aip.org/apl/copyright.jsp

[4]N. Biyikli, I. Kimukin, O. Aytur, E. Ozbay, IEEE Photon. Technol. Lett. **16**, 1718 (2004).
[5]T. Li, D. J. H. Lambert, A. L. Beck, C. J. Collins, B. Yang, J. M. M. Wong, U. Chowdhury, R.D. Dupuis and J. C. Campbell, Electron. Lett. **36**, 1581 (2000).
[6]K. A. McIntosh, R. J. Molnar, L. J. Mahoney, A. Lightfoot, M. W. Geis, K. M. Molvar, I. Melngailis, R. L. Aggarwal, W. D. Goodhue, S. S. Choi, D.L. Spears, and S. Verghese, Appl. Phys. Lett. **75**, 3485 (1999).
[7]J. C. Carrano, D. J. H. Lambert, C. J. Eiting, C. J. Collins, T. Li, S. Wang, B. Yang, A. L. Beck, R. D. Dupuis, and J. C. Campbell, Appl. Phys. Lett. **76**, 924 (2000).
[8]A. Osinsky, M. S. Shur, R. Gaska, and, Q. Chen, Electron. Lett. **34**, 691 (1998).
[9]S. Verghese, K. A. McIntosh, R. J. Molnar, L. J. Mahoney, R. L. Aggarwal, M. W. Geis, K. M. Molvar, E. K. Duerr, and I. Melngailis, IEEE Electron Device Lett. **48**, 502 (2001).
[10]K. A. McIntosh, R. J. Molnar, L. J. Mahoney, K. M. Molvar, N. Efremov, and S. Verghese, Appl. Phys. Lett. **76**, 3938 (2000).
[11]B. Yang, T. Li, K. Heng, C. Collins, S. Wang, J. C. Carrano, R. D. Dupuis, J. C. Campbell, M. J. Schurman, and I. T. Ferguson, IEEE J. Quantum Electron. **36**, 1389 (2000).

Downloaded 23 Nov 2005 to 139.179.96.116. Redistribution subject to AIP license or copyright, see http://apl.aip.org/apl/copyright.jsp